Molecular Genetics & Genomic Medicine

WILEY

Molecular Genetics & Genomic Medicine
Open Access

ORIGINAL ARTICLE OPEN ACCESS

Functional Characterization of a Novel Intronic Variant in *PIEZO2* in a Recessive Form of Distal Arthrogryposis With Impaired Proprioception and Touch (DAIPT)

Michela Bellardita[1] | Ferruccio Romano[2] | Ludovica Menta[1] | Joana Soraia Martinheira Da Silva[1] | Marzia Ognibene[3] | Simona Baldassari[1,3] | Marco Di Duca[3] | Chiara Panicucci[4] | Serena Baratto[4] | Noemi Brolatti[4] | Marina Pedemonte[5] | Chiara Fiorillo[1,6] | Claudio Bruno[1,4] | Marcello Scala[1,3] | Federico Zara[1,3] | Francesca Faravelli[2] | Francesca Madia[3] | Serena Cappato[3] | Renata Bocciardi[1,3] | Valeria Capra[2]

[1]DINOGMI—Department of Neuroscience, Rehabilitation, Ophthalmology, Genetics, Maternal and Child Health, University of Genoa, Genoa, Italy | [2]Genomics and Clinical Genetics Unit, IRCCS Istituto Giannina Gaslini, Genoa, Italy | [3]Medical Genetics Unit, IRCCS Istituto Giannina Gaslini, Genoa, Italy | [4]Centre of Translational and Experimental Myology, IRCCS Istituto Giannina Gaslini, Genoa, Italy | [5]Pediatric Neurology and Neuromuscular Disorders Unit, IRCCS Istituto Giannina Gaslini, Genoa, Italy | [6]Child Neuropsychiatry, IRCCS Istituto Giannina Gaslini, Genoa, Italy

Correspondence: Serena Cappato (serenacappato@gaslini.org)

Received: 17 March 2025 | **Revised:** 30 June 2025 | **Accepted:** 17 July 2025

Funding: This work was supported by the European Reference Network (ERN) "ITHACA" and the Italian Ministry of Health through the Ricerca corrente 2024.

Keywords: DAIPT | intronic variant | *PIEZO2* | splicing

ABSTRACT

Background: Distal arthrogryposis with impaired proprioception and touch (DAIPT) is a rare autosomal recessive neurological disease characterized by progressive alteration of mechanosensation. DAIPT is caused by loss of function variants in the *PIEZO2* gene that encodes an ionic channel involved in mechanotransduction signaling. Our study started from the case of an 11-year-old boy with skeletal and neuromuscular features suggestive of DAIPT.

Methods: Exome sequencing was performed on the trio. The identified variants in *PIEZO2* were validated by Sanger sequencing. Functional assays of the variants were performed by minigene assay in HEK-293 cells and on patient-derived cells using NMD inhibitors.

Results: Trio exome sequencing revealed the presence of two novel variants in the *PIEZO2* gene: a nonsense variant (c.1924G>T; p.Glu642*) and an intronic variant of uncertain significance (c.2170-15A>G). Functional analysis demonstrated that the intronic variant disrupts splicing, leading to premature stop codon formation and possible mRNA targeting to nonsense-mediated mRNA decay (NMD). Molecular study in patient-derived fibroblasts with specific NMD inhibitors shows that transcripts derived from both alleles are degraded by NMD, thus confirming the effect of the nonsense variant and enabling reclassification of the VUS.

Conclusion: We present the phenotypic and genetic description of a patient with features suggestive of DAIPT carrying novel biallelic variants in *PIEZO2*, one of which could be reclassified as pathogenic after functional assays. This study also provides a detailed review of all the published patients with DAIPT and expands the phenotypic and genetic understanding of DAIPT, aiding in diagnosis, genetic counseling, and clinical management.

Michela Bellardita, Ferruccio Romano, Francesca Madia, and Serena Cappato have contributed equally to this work.

Chiara Panicucci, Serena Baratto, Chiara Fiorillo, and Claudio Bruno are members of the European Reference Network for Neuromuscular Diseases (ERN-NMD).

1 | Introduction

PIEZO proteins are members of a large family of highly conserved mechanosensitive ion channels (MICs) that are involved in mechanotransduction by transforming mechanical stimuli into biochemical signals (He et al. 2024; Cox et al. 2019; García-Mesa et al. 2017). Two different PIEZO proteins, PIEZO1 and PIEZO2, are encoded by the corresponding genes *PIEZO1* (OMIM #611184) and *2* (OMIM #613629). *PIEZO1* (OMIM #611184) is mainly expressed in non-sensory organs like the lungs, bladder, and skin. It is involved in numerous cellular processes, including bone homeostasis, organogenesis, and regulation of blood flow (He et al. 2024; Fang et al. 2021).

PIEZO2 (OMIM #613629), mainly expressed in sensory tissues such as dorsal root ganglion (DRG) sensory neurons and Merkel cells (Fang et al. 2021), is involved in mechanosensation by playing an important role in mediating tactile sensations, motor coordination, and nociception (Sánchez-Carranza et al. 2024; Mahmud et al. 2017). Moreover, PIEZO2 is a detector of airway distension, which is essential to ensure effective breathing at birth and to maintain regular breathing in adulthood (al Balushi et al. 2023).

Differences in expression of PIEZO electric channels lead to different clinical conditions. Variants in the *PIEZO1* gene cause an autosomal dominant pleiotropic syndrome called Dehydrated Hereditary Stomatocytosis 1 (DHS1, OMIM #194380) characterized mostly by gain-of-function missense mutations that cause a slowdown in mechanosensitive channel activation, resulting in increased red blood cell membrane permeability and erythrocyte dehydration (Rosato et al. 2025; Zama et al. 2020). Biallelic loss-of-function variants in *PIEZO1* determine the recessive autosomal lymphatic malformation 6 (LMPHM6, OMIM #616843), a form of generalized lymphatic dysplasia (GLD) (Fotiou et al. 2015; Yamaguchi et al. 2019). *PIEZO2* is associated with several genetic diseases. Gain-of-function variants determine an increase in ion channel activity and are linked to three different types of arthrogryposis inherited as autosomal dominant conditions: Gordon syndrome or Distal Arthrogryposis Type 3 (OMIM #114300), Distal Arthrogryposis Type 5 (OMIM #108145) and Mardene-Walker syndrome (OMIM #248700) (Mahmud et al. 2017; Alhazmi et al. 2023; Coste et al. 2013), while loss-of-function variants cause Distal Arthrogryposis with Impaired Proprioception and Touch (DAIPT, OMIM #617146).

DAIPT, first described in 2016 (Chesler et al. 2016), is an autosomal recessive neurological disorder characterized by respiratory insufficiency and feeding difficulties in the neonatal period, short stature, scoliosis, congenital hip dysplasia, hypotonia, hand abnormalities, like camptodactyly, and foot abnormalities such as deformities, congenital talipes equinovarus, and pes planus. Currently, 26 DAIPT patients have been reported in the literature, most of whom are homozygous for loss-of-function variants due to consanguinity, although cases of compound heterozygosity have also been reported (Supplementary Table S1) (Delle Vedove et al. 2016; Behunova et al. 2019; Oakley-Hannibal et al. 2020; Klaniewska et al. 2021).

In this paper we report a patient with a clinical suspicion of DAIPT and two novel variants in *PIEZO2*: a nonsense pathogenic change (c.1924G>T) and an intronic variant with uncertain significance (VUS) (c.2170-15A>G) identified through exome sequencing, for which we provided a molecular characterization both in cellular-based assays and in the patient's primary cells.

2 | Results

2.1 | Case Description

We report a male patient, now aged 11 years old, first referred to our Institute at the age of 8 months because of hypotonia, neurodevelopmental delay, stridor, and feeding problems with failure to thrive. Clinical details and comparison with cases reported in the literature are summarized in Table 1. The child was born at 39 weeks and 6 days of gestation from non-consanguineous parents. Pregnancy was complicated by threatened abortion at 33 weeks. Delivery was spontaneous. Growth parameters at birth were within the normal range: weight was 3770 g (74th percentile, pc), length 50 cm (30th pc) and head circumference 33.5 cm (1st pc). APGAR scored 8 and 8. Soon after birth, for severe respiratory distress, the child was admitted to the intensive care unit (ICU). He also presented with global hypotonia, profuse sweating, poor suck, feeding difficulties, dysphagia, and limited spontaneous movements. Gavage feeding became necessary. For

TABLE 1 | Summary of the DAIPT associated clinical features.

Clinical features	This study	DAIPT patients reported in the literature (tot 27)
Neonatal respiratory distress	+	*14/18*
Hypotonia	+	*22/25*
Feeding difficulties	+	*14/21*
Motor delay	+	*27/27*
Cognitive delay	−	*4/26*
Absent deep tendon reflexes	−	*19/21*
Hand abnormalities	+	*22/27*
Foot abnormalities	+	*22/25*
Scoliosis	+	*20/22*
Hip dysplasia	−	*7/22*
Reduced proprioception	NA	*7/7*
Dysmorphic features	+	*14/20*
Short stature	+	*13/16*
Brain/Spine MRI	Normal	*3/11**

Abbreviations: DAIPT, distal arthrogryposis with impaired proprioception and touch; MRI, magnetic resonance imaging; NA, not available.
*Patients showing mild ventricular asymmetry, cavum septum pellucidum, or spinal anomalies at the MRI.

the occurrence of stridor, the patient underwent laryngoscopy demonstrating congenital laryngotracheomalacia. Some dysmorphic features were also observed. A few months later, the proband underwent surgery for right cryptorchidism. For transient hypercalciuria (not confirmed at follow-ups), ultrasound of the abdomen and urinary tract was performed, only identifying a longer right kidney.

The child exhibited delayed achievement of developmental milestones: head control was reached at 6 months, whereas autonomous walking was achieved at 3 years of age, with persisting gait imbalance, wide-based gait, and frequent falls.

The following dysmorphic features were described in the patient, including a flat facial profile with maxillozygomatic hypoplasia, myopathic facies, bitemporal narrowing, arched eyebrows, hypertelorism, palpebral angiomas, palpebral ptosis, anteverted nares, and hyperplasia of columella, thin upper lip vermilion, micrognathia, and high-arched palate, pointed chin, low-set ears, short neck, pectus excavatum, scoliosis, and short upper limbs (Figure 1, Table 1).

Skeletal deformities were characterized by a worsening course over time, being recognizable as a picture of distal arthrogryposis. Joint stiffness, especially at the scapulohumeral joint, and flexion contractures of distal phalanges of the third, fourth, and fifth fingers bilaterally, adduction of thumbs, clinodactyly, camptodactyly, bilateral bowed tibia, overlapping toes, and club feet were noticed. Laboratory investigations, including creatine kinase (CK), did not reveal any abnormalities. Sensory and motor nerve conduction velocities (NCV), performed at 8 months and repeated at 11 years, were normal.

An open muscle biopsy, performed at 11 months, showed nonspecific findings including moderate variation in fiber size, with several hypotrophic and rounded myofibers, mild increase in perimysial connective tissue, and minimal alterations in the myofibrillar network (Figure 2).

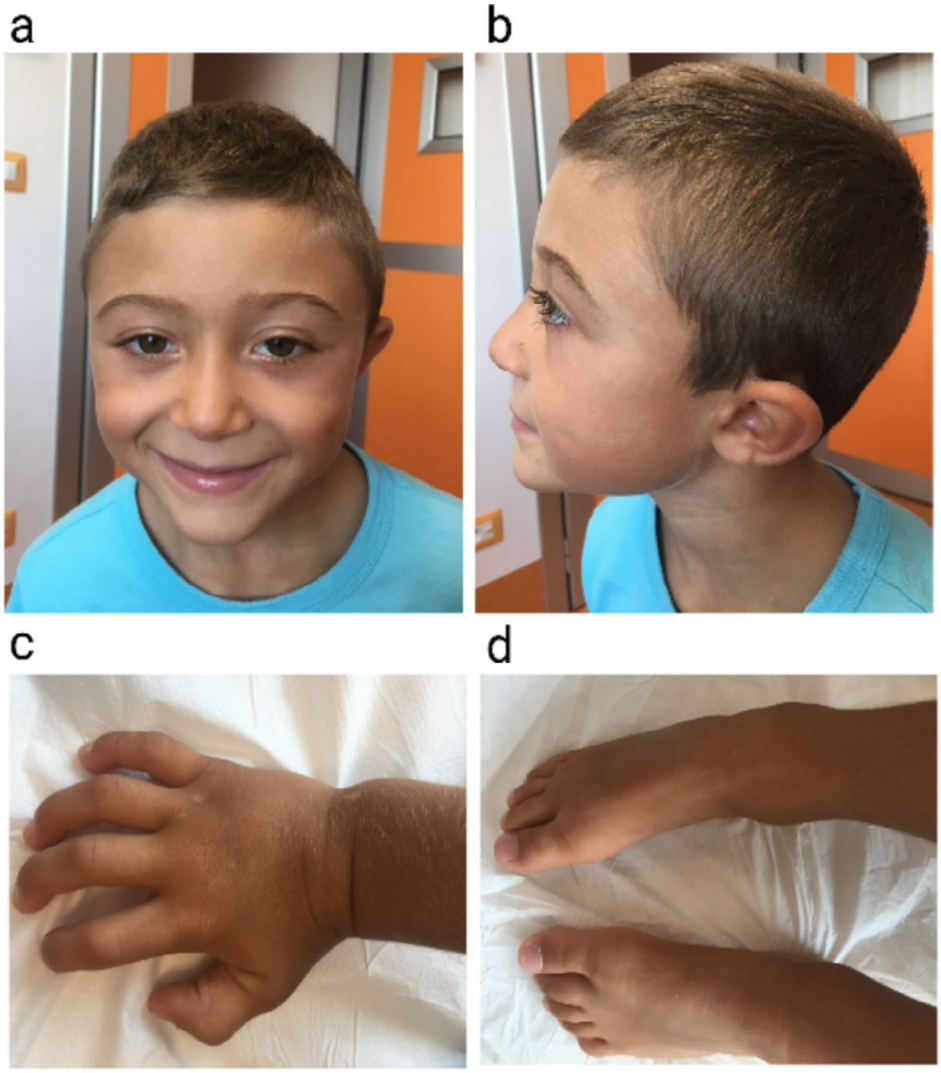

FIGURE 1 | Clinical presentation of the patient at the age of 5 years old. (a) facial appearance characterized by bitemporal narrowing of the forehead, ptosis, protruding columella, thin upper lip vermilion, pointed chin; (b) flat facial profile with zygomatic hypoplasia, and low-set ears. (c) right hand showing contractures of fingers; (d) feet with talipes equinovarus, more pronounced to the right. The appearance of hands and feet deformities has worsened over time.

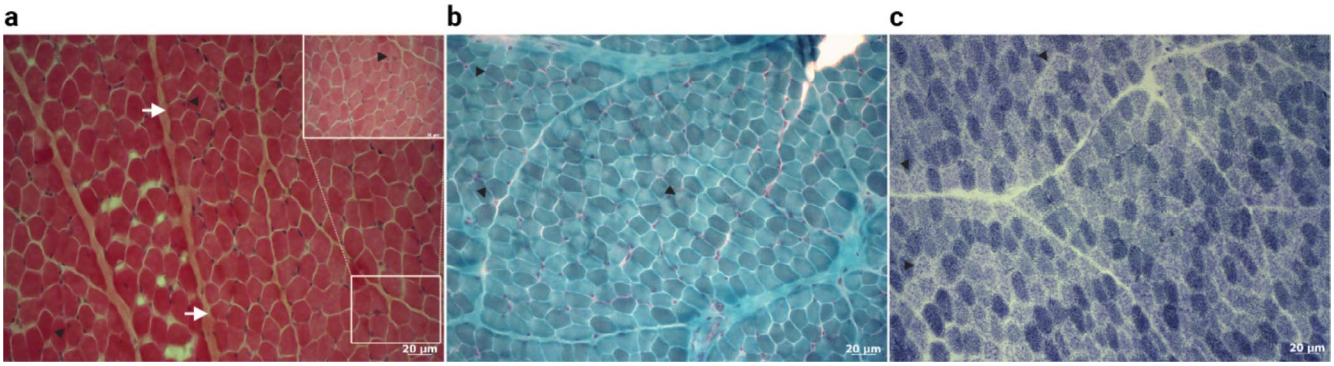

FIGURE 2 | Open muscle biopsy performed at 11 months. (a) Hematoxylin and Eosin (H&E) staining shows a moderate variability in fiber caliber, with the presence of several hypotrophic fibers with a rounded shape (white arrows). The percentage of centralized nuclei is within normal limits, although some nuclei with a vesicular appearance are noted (black arrow caps). Connective tissue is moderately increased, particularly in the perimysial area; (b) Gomori Trichrome (GT) staining reveals an increased fuchsinophilic punctate pattern in a considerable percentage of fibers (black arrow caps); (c) Nicotinamide adenine dehydrogenase (NADH)-tetrazolium reductase staining reveals minimal alterations in the myofibrillar network of several fibers, with no specific significance (black arrow caps).

At 5 years, brain and spine magnetic resonance imaging (MRI) scans were normal. At 6 years, cardiac ultrasound and ophthalmologic evaluations did not highlight pathologic signs.

At last examination, at 11 years, he reports easy fatigability when walking long distances or writing for extended periods; for this reason, he uses a postural stroller for longer trips and requires the assistance of a support teacher at school. Frequent falls and mild upper limb muscle weakness are reported. Clumsiness and poor fine motor coordination persist, in absence of cognitive delay.

The collection of family history highlighted that the proband's father had non progressive scoliosis, mild joint hypermobility, and bifid right thumb, while the proband's elder sibling was referred with scoliosis, treated with corset and minor signs like cupped ears, mild bilateral genu valgum, bilateral pes planus, joint laxity, in absence of any functional limitation, psychomotor delay or cognitive issues (Figure S1). It is worth noticing that the mother reported four miscarriages, all in the first trimester of pregnancy (see Figure S1). Methylation analysis for Prader-Willi/Angelman syndrome and Diepoxybutane (DEB) analysis were performed in the proband, with normal results.

During the following clinical genetics evaluation, the family was proposed a trio whole exome sequencing (ES) analysis.

2.2 | Molecular Diagnosis

Biological samples from the patient and his parents were obtained after written informed consent from proband's parents. ES was performed in all subjects, and the analysis revealed the presence of two novel variants of *PIEZO2* (RefSeq NM_001378183.1; NP_001365112.1): a nonsense variant (c.1924G>T; p.Glu642*; dbSNP, rs1598482405, exon 15), classified as Pathogenic, Class 5 (PVS1, PM2, PP5) (https://franklin.genoox.com), according to the ACMG criteria (Richards et al. 2015), inherited from the mother; an intronic substitution (c.2170-15A>G; dbSNP, rs934167990, IVS 15), classified as VUS (PM2) (https://franklin.genoox.com), according to the ACMG criteria (Richards et al. 2015), inherited from the father.

No other pathogenic or likely pathogenic variants were detected in *PIEZO2* or other genes. As shown in Figure 3, the presence of the two variants was confirmed by Sanger sequencing.

The *in silico* analysis of the c.2170-15A>G variant with SpliceAI (Jaganathan et al. 2019) and Human Splicing Finder (Desmet et al. 2009) predicted the impairment of the canonical acceptor site of exon 16 with the generation of a new splicing site. Therefore, the adjacent 14 intronic nucleotides are included in the coding sequence of exon 16, causing a frameshift and the generation of a premature stop codon after 45 bp. The presence of an early termination codon may trigger a nonsense-mediated mRNA decay (NMD) of the carrying transcript. We thus decided to explore the effect of this variant by functional validation.

2.3 | The c.2170-15A>G Variant Alters the Splicing of *PIEZO2* mRNA

To characterize the intronic variant, we performed the minigene assay. This approach is based on the use of the pSPL3 vector (Burn et al. 1995; Duyk et al. 1990), a plasmid designed for exon trapping and suitable for splicing analysis. We subcloned into the pSPL3 a PCR product including exon 16 of the *PIEZO2* gene and the intronic flanking regions, wild-type or carrying the c.2170-15A>G variant.

The different plasmids were transiently transfected in Hek-293 for 24 h, and the total RNA was extracted to perform RT-PCR with oligonucleotides specifically designed for the vector-derived exons SD and SA.

Figure 4a shows the band corresponding to the splicing of the minigene derived from the empty vector (size 263 bp) and two higher bands with a similar size deriving from the splicing of the wild type (WT) or mutated (Var) minigenes carrying exon 16 of *PIEZO2*. The sequence analysis demonstrated that, in accordance with the *in silico* predictions, the c.2170-15A>G substitution alters the splicing by including 14 nucleotides of intron 15 into the exon 16 coding sequence (Figure 4b).

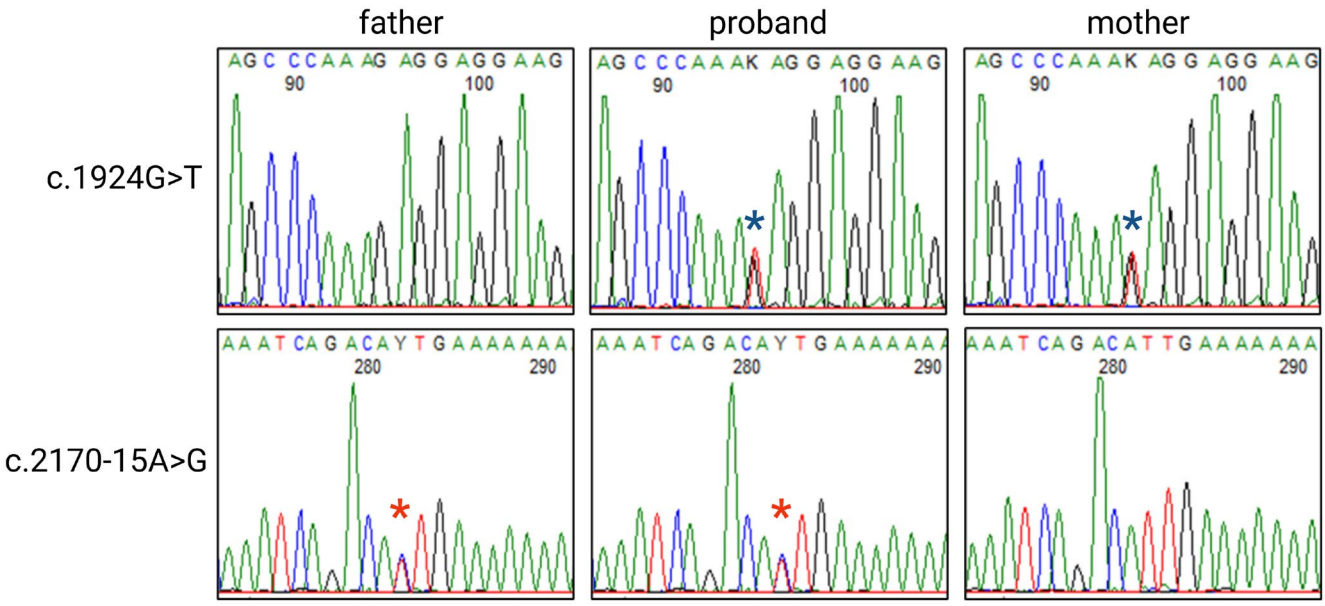

FIGURE 3 | Identification of two novel variants of *PIEZO2*. Details of Sanger sequences of the two variants identified in the *PIEZO2* gene in the proband and his parents.

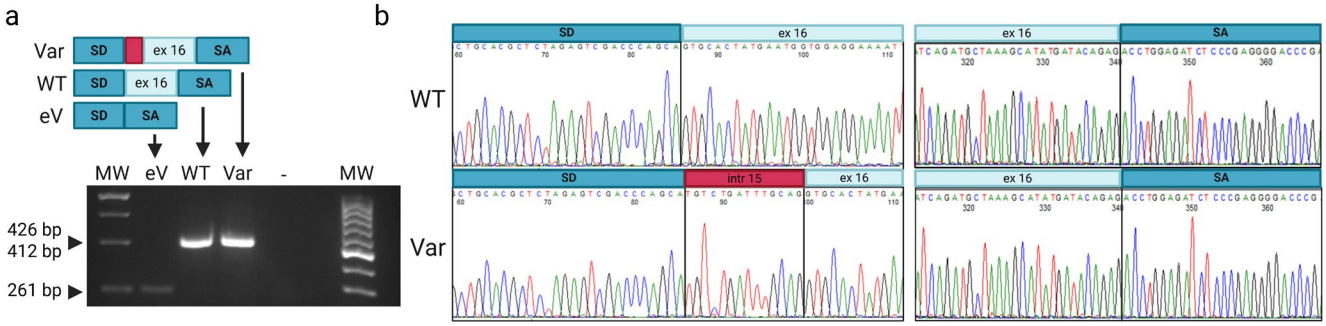

FIGURE 4 | The c.2170-15A>G variant alters the splicing of *PIEZO2* exon 16. (a) Schematic representation of the PCR products obtained by the amplification of the cDNA retro-transcribed from RNA extracted of Hek-293 cells transfected 24 h with the following pSPL3 vectors: EV, empty vector; WT, pSLP3 vector with wild type *PIEZO2* exon 16 and Var, pSLP3, the vector carrying the variant in *PIEZO2* intron 15. Vector exons SD and SA were indicated in light blue, *PIEZO2* exon 16 is shown in sky blue and the 14 nucleotides of introns 15 are represented by a red rectangle. The agarose gel electrophoresis of PCR products obtained by the amplification with SD6 and SA2 oligonucleotides is reported in the bottom panel, the corresponding sizes are indicated on the left. (b) Details of the Sanger sequences of minigenes transcripts at the junction between SD/exon16, and exon 16/SA in the WT and Var minigene. MW, molecular weight marker ladders, 1 kb on the left and 100 kb on the right; – no template control. Image created with Biorender.com.

2.4 | The Identified Variants Target *PIEZO2* mRNA to NMD-Mediated Degradation in Primary Patients' Cells

The minigene strategy confirmed that the intronic variant generates a new acceptor splicing site that masks the usage of the canonical one. This prompted us to verify this observation on *PIEZO2* mRNA obtained in the patient's primary cells. We obtained a skin biopsy and isolated a dermal fibroblast culture. As both the identified variants lead to the generation of early stop codons that may target the mutated transcripts to NMD, we treated the patient's cells with two different NMD inhibitor agents, Cycloheximide (Chx, 100 μg/mL) and Puromycin (Puro, 200 μg/mL) (Carter et al. 1995).

As shown in Figure 5a, *PIEZO2* transcripts are not detectable in patient's skin fibroblasts (indicated as NT) as the *PIEZO2* mRNAs generated by both the variant alleles are targeted to NMD. The treatment with NMD inhibitors rescues the transcripts from degradation, allowing the detection of *PIEZO2* specific RT-PCR products (Figure 5b).

3 | MATHERIAL and METODS

3.1 | Ethical Compliance

This study was conducted in accordance with the Declaration of Helsinki, and ethics approval was obtained from the medical ethical committee installed by Gaslini Children's Hospital (Comitato Etico Territoriale della Regione Liguria, approval code: CER Liguria 399/2021). Written informed consent was obtained from parents for clinical testing and publication of genetic and clinical data, as well as clinical photographs.

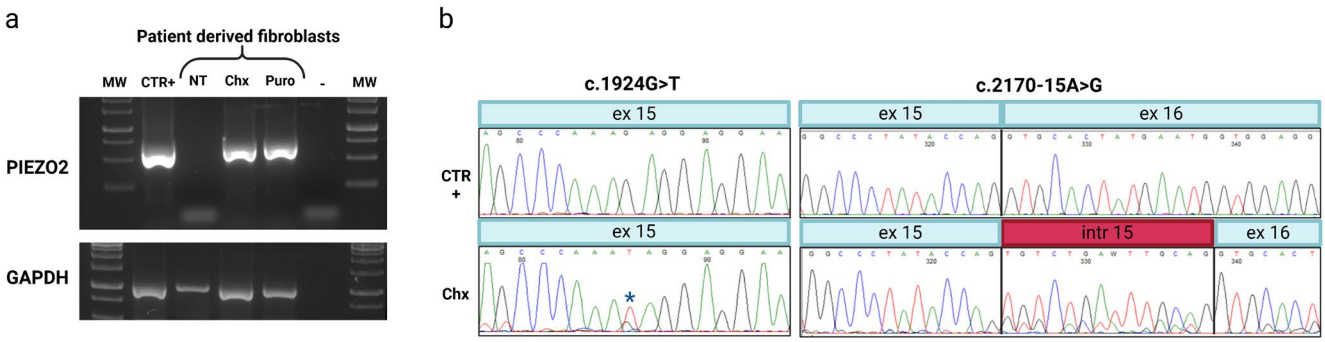

FIGURE 5 | The identified variants target the *PIEZO2* mRNA to NMD in patient's primary fibroblasts. (a) PCR products obtained by the amplification of cDNA derived from patient's fibroblasts treated with 100 μg/mL of Cycloheximide (Chx) or 200 μg/mL of Puromycin (Puro). CTR+ cDNA derived from RNA extracted from human dermal fibroblasts used as positive control. GAPDH was used as housekeeping gene to check the efficiency of the cDNA synthesis. (b) Details of Sanger sequencing of the cDNA, focusing on exon 15 and of the region spanning from exons 15 and 16. Blue asterisk indicates the variant inherited from the mother and the red area represent the insertion of 14 nt of intron 15 into the transcript due to the splicing variant inherited from the father. MW, Molecular Weight 1 Kb. Image created with Biorender.com.

3.2 | Molecular Diagnosis

Exome Sequencing (ES) was performed on all the members of the family using genomic DNA extracted from peripheral blood. ES was performed using an in-house analysis platform according to the BWA/GATK's based pipelines (GATK Best Practices, https://gatk.broadinstitute.org/). Targeted Sanger sequencing using standard methods was also performed for validation of identified variants and segregation analysis. After filtering for allele frequency (≤0.01% in public databases, including GnomAD v2.1.1; https://gnomad.broadinstitute.org/), candidate variants were screened according to family segregation, conservation (GERP score), predicted impact on protein function through *in silico* tools (including SIFT, PolyPhen-2, Mutation Taster, AlphaMissense), and presence in clinical databases (ClinVar). Candidate variants were classified (https://franklin.genoox.com/) according to the American College of Medical Genetics and Genomics (ACMG) criteria (Richards et al. 2015). *PIEZO2* variants are listed according to the transcript NM_001378183.1 and referred to the hg38/GRCh38 assembly. Informed consent for the publication of clinical and genetic data was obtained from all participants.

3.3 | Plasmids' Construction

To study the effect of the intronic variant on the splicing mechanism, the minigene assay based on the pSPL3 exon trapping vector was applied (Burn et al. 1995; Duyk et al. 1990). The plasmid was already available in the lab. A fragment of 501 bp, including exon 16 of *PIEZO2* and the intronic flanking regions (chr18:10786868-10787368; GRCh38/hg38) was amplified by PCR (GoTaq Master mix, Promega, Wisconsin, USA) from the proband's father.

The obtained PCR products were cloned in the pCR 2.1-TOPO TA (TOPO TA Cloning, Invitrogen) and clones were checked by direct sequencing to verify and isolate both the WT and the mutated alleles. Finally, the fragments under analysis were subcloned into the splicing vector pSPL3 (pSPL3-ex16 WT and pSPL3-ex16 mut) in the *EcoRI* restriction site and checked by sequencing.

3.4 | Cell Cultures, Transient Transfection and Minigene Assay

Patient's derived fibroblasts were obtained by skin biopsy upon administration of a specific informed consent and cultured in RPMI medium, containing 20% fetal bovine serum (FBS, Gibco, Thermo Fisher Scientific, Massachusetts, USA).

The Human Dermal Fibroblasts (HDFa) were purchased from Gibco and routinely cultured in complete RPMI medium, containing 16% FBS.

The Hek-293 cell line was already available in the laboratory, previously purchased by ATCC. Cells were routinely cultured in complete medium consisting of Essential Modified Medium (MEM) with 10% FBS. Cells were maintained at 37°C in a humidified atmosphere with 5% CO_2.

Transfection for minigene assay was performed in 6-well plates, by seeding 5×10^5/well Hek-293 cells on Day 0. The next day, cells were transfected with a mix composed of 2 μg of pSPL3-eV or pSPL3 PIEZO2 ex16 WT or pSPL3 PIEZO2 ex16 MUT, using the Lipofectamine 2000 reagent protocol (Invitrogen, Thermo Fisher Scientific, Massachusetts, USA). Twenty-four hours later, cells were lysed and processed for RNA extraction.

3.5 | Inhibition of the Nonsense-Mediated mRNA Decay

To inhibit the nonsense-mediated mRNA decay, patient-derived fibroblasts were treated for 6 h with 100 μg/mL of Cycloheximide (CAS n°66-81-9, Sigma-Aldrich) or overnight with 200 μg/mL of Puromycin (CAS n°58-58-2, InvivoGen, France). Cells were then lysed and RNA was extracted with the RNeasy plus Mini Kit (Qiagen, Germany) as suggested by the manufacturer.

3.6 | cDNA Retrotranscription

The *PIEZO2* cDNA was obtained by the retro-transcription of respectively 1 μg (for minigene assay) and 2 μg (for primary

cells) of total RNA by using Advantage RT-for-PCR (Takara, Shiga, Japan) and subsequently amplified by GoTaq Master mix (Promega, Wisconsin, USA) according to the manufacturer's protocol.

The PCR products were checked on 1.5% Agarose gel and cleaned up by Exo/SAP-IT (Thermo Scientific, Massachusetts, USA) digestion. Sequences were obtained with the Big Dye Terminator Cycle Sequencing Kit according to the provided protocol and run on a 3130xl Genetic Analyzer (Thermo Scientific, Massachusetts, USA). The analysis of the sequences was performed by the Sequencer 4.7 software (GeneCodes). Oligonucleotide sequences are available upon request.

3.7 | *In Silico* Study Analysis

The intronic variant described in this work was analyzed by SpliceAI (Jaganathan et al. 2019) and Human Splicing Finder (HSF, free license for academic users) (Desmet et al. 2009) bioinformatic tools designed to predict the potential effects on splicing. "Lollipop" plot was generated by using R-Project software (Version 4.4.0, www.r-project.org).

4 | Discussion

DAIPT is a rare autosomal recessive neurological disorder characterized by impaired proprioception and touch, ataxia, difficulty walking, dysmetria, muscle weakness and atrophy, and progressive skeletal contractures. Patients develop symptoms in early childhood. Here we describe the case of a proband with a complex phenotype characterized by perinatal respiratory distress, feeding difficulties, global hypotonia, motor delay, dysmorphic features (flat and myopathic face, thin upper lip, high-arched palate and short neck) in addition to progressive skeletal deformities (distal arthrogryposis, flexion deformity of thumbs and fingers, congenital talipes equinovarus, scoliosis) and neuromuscular deficits (gait imbalance, poor fine motor coordination and muscle weakness, especially at the upper limbs). Muscle biopsy showed mild nonspecific abnormalities as previously reported (Yamaguchi et al. 2019; Klaniewska et al. 2021; Haliloglu et al. 2017). The phenotype suggested a clinical suspicion of DAIPT.

The ES analysis of the trio leads to the identification of two previously unreported variants in *PIEZO2*: the nonsense variant c.1924G>T (p.Glu642*) and the intronic substitution c.2170-15A>G. The identification of these variants in our patient supported the clinical hypothesis of DAIPT (al Balushi et al. 2023; Klaniewska et al. 2021), a rare neuromuscular and skeletal syndrome associated with biallelic variants in the *PIEZO2* gene. Alongside the typical features of the condition, the patient presented with cryptorchidism and mild congenital anomalies of the kidney, which have not been described in DAIPT but are reported in association with *PIEZO2* variants in the HPO database (https://hpo.jax.org/browse/gene/NCBIGene:63895). Moreover, the patient experienced laryngotracheomalacia in the neonatal period, which has not been reported in association with this condition, to our knowledge. Further studies are needed to infer clearer information about a possible expansion of the DAIPT phenotypic "spectrum", given the limited number of reported cases and the relative frequency of laryngomalacia in infants. Cognitive delay is reported only in a minority of affected individuals (al Balushi et al. 2023; Klaniewska et al. 2021). The patient's clinical features are summarized in comparison to previously reported DAIPT cases in Table 1. For a more detailed summary of reported clinical features, see Supplementary Table S1.

Nonsense variants or small delins generating early STOP codons represent the most common alteration of the *PIEZO2* gene. Few splicing variants affecting canonical donor or acceptor sites of the gene have also been reported in the literature (Figure 6 and Table S2) (Mahmud et al. 2017; al Balushi et al. 2023; Delle Vedove et al. 2016; Haliloglu et al. 2017) and classified as Pathogenic/Likely Pathogenic according to the ACMG criteria, but no functional evidence was provided (Table S2).

Here we provide evidence of the deleterious effect of the variant c.2170-15A>G initially considered as VUS. The variant alters the sequence adjacent to the exon/intron boundary and affects the usage of the canonical splicing site, thus impairing mRNA processing. This was experimentally validated by the minigene approach and by cDNA analysis in the patient's primary cells, demonstrating that the substitution causes the generation of a frameshift in the *PIEZO2* mRNA with the formation of an early stop codon. We provide evidence that both the variants identified in the proband cause the degradation of *PIEZO2* mRNA that is not detectable in the patient's primary fibroblasts. The treatment

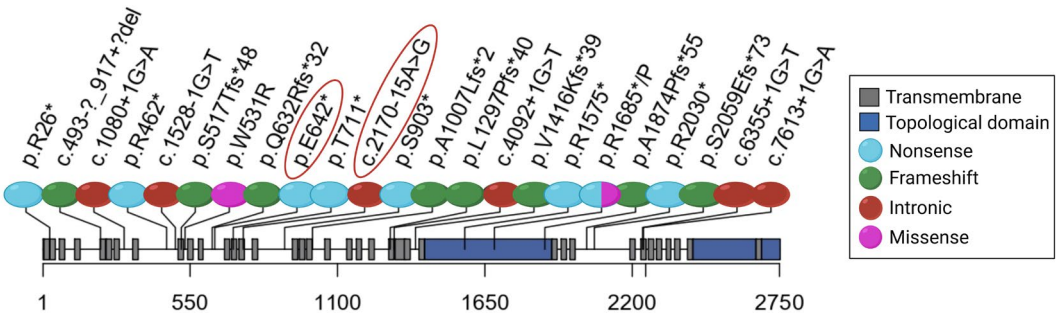

FIGURE 6 | *PIEZO2* variants associated with DAIPT. The "lollipop" diagram illustrates the position of all the variants in *PIEZO2* associated with DAIPT so far. Transmembrane domains are indicated in gray and the topological domains in blue. The variants reported are nonsense (light blue), frameshift (green), intronic (red) and missense (pink). The mutations identified in this study are circled in red. Numbers reported on the black line indicate amino acid positions. Data used to generate this chart are provided in the Table S3.

of cells with known NMD inhibitors restored the expression of the aberrant *PIEZO2* transcripts, confirming that these mRNAs are degraded by this process.

We highlight the importance of functional studies in reclassifying the intronic VUS c.2170-15A>G, which was demonstrated to cause a deleterious effect, thus enabling the genetic diagnosis of DAIPT in our patient, for having biallelic *PIEZO2* damaging variants. Hence, genetic counseling for the patient and his family could benefit from this functional reclassification, as the carrier parents were provided with clear-cut information on the reproductive risk for following pregnancies.

The clinical management of the proband per se has improved, since the child is undergoing complete multidisciplinary evaluations to promptly address any other possible DAIPT clinical manifestation. To our knowledge, no internationally recognized surveillance programs are available, and the principal issues to clinically address or monitor seem to be represented by the skeletal and neuromuscular anomalies. In the HPO database, also genitourinary and cardiac anomalies are reported in association with *PIEZO2* variants, like cryptorchidism, inguinal herniation, hydronephrosis, kidney hypoplasia or dysplasia, and hydroureter. Among cardiologic anomalies, abnormal cardiac morphology and ventricular septal defect can be present.

Although these manifestations occur rarely, we highlight the importance of conducting cardiologic and urogenital evaluations following the initial diagnosis by cardiac and urinary tract (US) ultrasound, to timely address these possible manifestations. It is equally important to have a multidisciplinary approach with the goal of increasing the chances of identifying the underlying genetic basis.

In conclusion, we provide a detailed phenotypic and genetic description of a patient with features suggestive of DAIPT, carrying novel biallelic pathogenic variants in *PIEZO2*, one of which could be reclassified as pathogenic after functional assays. This study will be helpful for physicians and researchers dealing with this complex and rare syndrome, ameliorating clinical management for patients and families.

Author Contributions

Michela Bellardita: functional studies, manuscript writing. Ferruccio Romano: medical consultation, manuscript writing, critical revision. Ludovica Menta, Joana Soraia Martinheira Da Silva: functional studies, manuscript revision. Marzia Ognibene, Simona Baldassari, Marco Di Duca: technical support to the functional studies. Serena Baratto: muscle biopsy evaluation. Chiara Fiorillo: skin and muscle biopsy and medical consultation. Chiara Panicucci, Noemi Brolatti, Marina Pedemonte, Chiara Fiorillo, Claudio Bruno: medical consultation, patient's clinical management. Francesca Madia: molecular diagnosis, manuscript revision. Marcello Scala, Federico Zara, Francesca Faravelli: critical reading of the manuscript. Renata Bocciardi, Serena Cappato: conceptualization, manuscript writing, and revision; Valeria Capra: medical consultation, patient's clinical management, manuscript revision.

Acknowledgments

We thank the family for the kind availability to participate in this study. Genetic analysis and functional experiments were supported in part by the European Reference Network (ERN) "ITHACA" and by Ricerca corrente 2024 of the Italian Ministry of Health. Open access funding provided by BIBLIOSAN.

References

al Balushi, A., M. al Hinai, A. Al Hosni, et al. 2023. "Distal Arthrogryposis With Impaired Proprioception and Touch: A Novel Variant in *PIEZO2* Gene in Omani Patients and a Genotype-Phenotype Review From a Single-Center Experience." *Journal of Pediatric Genetics* 13, no. 3: 175–180. https://doi.org/10.1055/s-0043-1764127.

Alhazmi, W., A. Qurban, and E. Alrashidi. 2023. "Case Report of Generalized Lymphatic Dysplasia With PIEZO1 Mutation and Review of the Literature." *Respiratory Medicine Case Reports* 44: 101872. https://doi.org/10.1016/j.rmcr.2023.101872.

Behunova, J., M. Gerykova Bujalkova, G. Gras, et al. 2019. "Distal Arthrogryposis With Impaired Proprioception and Touch: Description of an Early Phenotype in a Boy With Compound Heterozygosity of PIEZO2 Mutations and Review of the Literature." *Molecular Syndromology* 9, no. 6: 287–294. https://doi.org/10.1159/000494451.

Burn, T. C., T. D. Connors, K. W. Klinger, and G. M. Landes. 1995. "Increased Exon-Trapping Efficiency Through Modifications to the pSPL3 Splicing Vector." *Gene* 161, no. 2: 183–187. https://doi.org/10.1016/0378-1119(95)00223-s.

Carter, M. S., J. Doskow, P. Morris, et al. 1995. "A Regulatory Mechanism That Detects Premature Nonsense Codons in T-Cell Receptor Transcripts In Vivo Is Reversed by Protein Synthesis Inhibitors in Vitro." *Journal of Biological Chemistry* 270, no. 48: 28995–29003. https://doi.org/10.1074/jbc.270.48.28995.

Chesler, A. T., M. Szczot, D. Bharucha-Goebel, et al. 2016. "The Role of PIEZO2 in Human Mechanosensation." *New England Journal of Medicine* 375, no. 14: 1355–1364. https://doi.org/10.1056/NEJMoa1602812.

Coste, B., G. Houge, M. F. Murray, et al. 2013. "Gain-Of-Function Mutations in the Mechanically Activated Ion Channel PIEZO2 Cause a Subtype of Distal Arthrogryposis." *Proceedings of the National Academy of Sciences of the United States of America* 110, no. 12: 4667–4672. https://doi.org/10.1073/pnas.1221400110.

Cox, C. D., N. Bavi, and B. Martinac. 2019. "Biophysical Principles of Ion-Channel-Mediated Mechanosensory Transduction." *Cell Reports* 29, no. 1: 1–12. https://doi.org/10.1016/j.celrep.2019.08.075.

Delle Vedove, A., M. Storbeck, R. Heller, et al. 2016. "Biallelic Loss of Proprioception-Related PIEZO2 Causes Muscular Atrophy With Perinatal Respiratory Distress, Arthrogryposis, and Scoliosis." *American Journal of Human Genetics* 99, no. 6: 1406–1408. https://doi.org/10.1016/j.ajhg.2016.11.009.

Desmet, F. O., D. Hamroun, M. Lalande, G. Collod-Béroud, M. Claustres, and C. Béroud. 2009. "Human Splicing Finder: An Online Bioinformatics Tool to Predict Splicing Signals." *Nucleic Acids Research* 37, no. 9: e67. https://doi.org/10.1093/nar/gkp215.

Duyk, G. M., S. W. Kim, R. M. Myers, and D. R. Cox. 1990. "Exon Trapping: A Genetic Screen to Identify Candidate Transcribed Sequences in Cloned Mammalian Genomic DNA." *Proceedings of the National Academy of Sciences of the United States of America* 87, no. 22: 8995–8999. https://doi.org/10.1073/pnas.87.22.8995.

Fang, X. Z., T. Zhou, J. Q. Xu, et al. 2021. "Structure, Kinetic Properties and Biological Function of Mechanosensitive Piezo Channels." *Cell & Bioscience* 11, no. 1: 13. https://doi.org/10.1186/s13578-020-00522-z.

Fotiou, E., S. Martin-Almedina, M. A. Simpson, et al. 2015. "Novel Mutations in PIEZO1 Cause an Autosomal Recessive Generalized Lymphatic Dysplasia With Non-Immune Hydrops Fetalis." *Nature Communications* 6, no. 1: 8085. https://doi.org/10.1038/ncomms9085.

García-Mesa, Y., J. García-Piqueras, B. García, et al. 2017. "Merkel Cells and Meissner's Corpuscles in Human Digital Skin Display Piezo2

Immunoreactivity." *Journal of Anatomy* 231, no. 6: 978–989. https://doi.org/10.1111/joa.12688.

Haliloglu, G., K. Becker, C. Temucin, et al. 2017. "Recessive PIEZO2 Stop Mutation Causes Distal Arthrogryposis With Distal Muscle Weakness, Scoliosis and Proprioception Defects." *Journal of Human Genetics* 62, no. 4: 497–501. https://doi.org/10.1038/jhg.2016.153.

He, H., J. Zhou, X. Xu, P. Zhou, H. Zhong, and M. Liu. 2024. "Piezo Channels in the Intestinal Tract." *Frontiers in Physiology* 15: 1356317. https://doi.org/10.3389/fphys.2024.1356317.

Jaganathan, K., S. Kyriazopoulou Panagiotopoulou, J. F. McRae, et al. 2019. "Predicting Splicing From Primary Sequence With Deep Learning." *Cell* 176, no. 3: 535–548.e24. https://doi.org/10.1016/j.cell.2018.12.015.

Klaniewska, M., M. Jedrzejowska, M. Rydzanicz, et al. 2021. "Case Report: Further Delineation of Neurological Symptoms in Young Children Caused by Compound Heterozygous Mutation in the PIEZO2 Gene." *Frontiers in Genetics* 12: 620752. https://doi.org/10.3389/fgene.2021.620752.

Mahmud, A. A., N. A. Nahid, C. Nassif, et al. 2017. "Loss of the Proprioception and Touch Sensation Channel PIEZO2 in Siblings With a Progressive Form of Contractures." *Clinical Genetics* 91, no. 3: 470–475. https://doi.org/10.1111/cge.12850.

Oakley-Hannibal, E., N. Ghali, F. M. Pope, et al. 2020. "A Neuromuscular Disorder With Homozygosity for PIEZO2 Gene Variants: An Important Differential Diagnosis for Kyphoscoliotic Ehlers-Danlos Syndrome." *Clinical Dysmorphology* 29, no. 1: 69–72. https://doi.org/10.1097/MCD.0000000000000304.

Richards, S., N. Aziz, S. Bale, et al. 2015. "ACMG Laboratory Quality Assurance Committee. Standards and Guidelines for the Interpretation of Sequence Variants: A Joint Consensus Recommendation of the American College of Medical Genetics and Genomics and the Association for Molecular Pathology." *Genetics in Medicine* 17, no. 5: 405–424. https://doi.org/10.1038/gim.2015.30.

Rosato, B. E., V. D'Onofrio, R. Marra, et al. 2025. "RAS Signaling Pathway Is Essential in Regulating PIEZO1-Mediated Hepatic Iron Overload in Dehydrated Hereditary Stomatocytosis." *American Journal of Hematology* 100, no. 1: 52–65. https://doi.org/10.1002/ajh.27523.

Sánchez-Carranza, O., S. Chakrabarti, J. Kühnemund, et al. 2024. "Piezo2 Voltage-Block Regulates Mechanical Pain Sensitivity." *Brain* 147, no. 10: 3487–3500. https://doi.org/10.1093/brain/awae227.

Yamaguchi, T., K. Takano, Y. Inaba, et al. 2019. "PIEZO2 Deficiency Is a Recognizable Arthrogryposis Syndrome: A New Case and Literature Review." *American Journal of Medical Genetics. Part A* 179, no. 6: 948–957. https://doi.org/10.1002/ajmg.a.61142.

Zama, D., G. Giulietti, E. Muratore, et al. 2020. "A Novel PIEZO1 Mutation in a Patient With Dehydrated Hereditary Stomatocytosis: A Case Report and a Brief Review of Literature." *Italian Journal of Pediatrics* 46, no. 1: 102. https://doi.org/10.1186/s13052-020-00864-x.

Supporting Information

Additional supporting information can be found online in the Supporting Information section. **Figure S1.** Pedigree of the reported family. Grey symbol represents the DAIPT affected individual, and the arrow indicates the proband. Carrier parents are identified by a dot in the center of the symbol shape. **Table S1. Table S2. Table S3.**